Effective exponents in the long-range critical wetting of alkanes on aqueous substrates

Volker C. Weiss,[1,*] Emanuel Bertrand,[2,3,4] Salima Rafaï,[5] Joseph O. Indekeu,[6] and Daniel Bonn[7]
[1]*Eduard-Zintl-Institut für Anorganische und Physikalische Chemie, Technische Universität Darmstadt, Petersenstrasse 20, 64287 Darmstadt, Germany*
[2]*Liquides Ioniques et Interfaces Chargées, Université Pierre et Marie Curie–Paris 6, UMR 7612, 4 place Jussieu, Paris Cedex 05, 75252 Paris, France*
[3]*CNRS, UMR 7612, 75005 Paris, France*
[4]*ESPCI, UMR 7612, ParisTech, 75005 Paris, France*
[5]*Van der Waals–Zeeman Instituut, Valckenierstraat 65, 1018 XE Amsterdam, The Netherlands*
[6]*Instituut voor Theoretische Fysica, Katholieke Universiteit Leuven, B-3001 Leuven, Belgium*
[7]*Laboratoire de Physique Statistique de l'ENS, 24 rue Lhomond, 75231 Paris, France*
(Received 12 July 2007; published 19 November 2007)

Alkanes on water show a two-stage wetting transition. Upon raising the temperature, a first-order transition from a molecularly thin to a mesoscopically thick liquid film is followed by a continuous divergence of the film thickness. This second transition is brought about by long-range interactions between adsorbate and substrate and is, therefore, referred to as long-range critical wetting. The divergence of the film thickness is theoretically expected to occur according to the asymptotic power law $l \sim (T_{w,c}-T)^{\beta_s}$, with $\beta_s=-1$. This value has indeed been found for pentane on pure water; however, for hexane on salt solutions of different concentrations, $\beta_s=-0.73$ was found for a 1.5*M* solution of NaCl and $\beta_s=-0.57$ for a 2.5*M* salt solution. In addition, for hexane on a 2.5*M* solution of NaCl, an exponent of $\alpha_s=0.1$ was found from contact-angle measurements, differing greatly from the theoretically expected value of $\alpha_s=-1$. Using Dzyaloshinskii-Lifshitz-Pitaevskii theory, we calculate effective local exponents in order to explain the experimental findings. Taking into account the uncertainty of the exponents derived from experiments as well as the temperature range in which the measurements were carried out, a reasonable agreement between theory and experiment is found, thereby providing a consistent approach to resolving the apparently anomalous behavior of hexane on brine. The experimentally observed exponents $\beta_s=-0.57$ and $\alpha_s=0.1$ are also compatible with a long-range tricritical wetting transition, which is characterized by $\beta_s=-1/2$ and $\alpha_s=0$; this alternative explanation of the experimental findings is neither supported nor completely ruled out by our calculations.

DOI: 10.1103/PhysRevE.76.051602 PACS number(s): 68.08.Bc, 05.70.Jk, 68.35.Rh

I. INTRODUCTION

The scenario of sequential wetting is shown by alkanes of medium chain length on aqueous substrates, such as pure water and solutions of salt (NaCl) and of glucose [1–4]. In such a scenario, the liquid phase of the alkane (typically pentane, hexane, or heptane), which is in equilibrium with its vapor phase, may cover the substrate in one of three (instead of the usual two) different ways. At low temperatures, the substrate surface is covered only partially by discrete droplets of the liquid adsorbate phase. These droplets exhibit a finite, nonzero contact angle with the substrate surface and are interconnected only by a molecularly thin layer of adsorbed alkane molecules. This wetting state is referred to as partial wetting and can be observed below the temperature $T_{w,1}$, to be specified below. Upon raising the temperature beyond $T_{w,1}$, the film thickness (of the film connecting the droplets) shows a discontinuous increase, which represents a first-order transition. Unlike in the usual first-order wetting, this transition does not lead directly to complete wetting, but to a wetting state which is called "frustrated complete wetting" [5], because the substrate surface is completely covered by the adsorbate film (as in the complete wetting state), but the contact angle is still nonzero and the wetting film has only a mesoscopic thickness of about 100 Å, whereas a true wetting layer is macroscopically thick. Once the system is in the frustrated complete wetting state, the film thickness varies continuously upon increase of the temperature and diverges as the critical wetting transition temperature $T_{w,c}$ is approached. Above $T_{w,c}$, the system is in the complete wetting state, which is characterized by a zero contact angle and a macroscopic film thickness. A similar sequence of wetting transitions was observed for a mixture of hexane and propane on water upon raising the pressure by injection of gaseous propane at constant temperature [6]. In a related study, the spreading of hydrocarbons on water was facilitated by injecting carbon dioxide, methane, or nitrogen [7].

The sequential-wetting scenario described in the preceding paragraph differs from the usual wetting transition from partial to complete wetting by the presence of an intermediate wetting state. The existence of the frustrated complete wetting state is made possible by an interplay of short- and long-range forces between the substrate and the adsorbate. Whereas the common first-order wetting transition from partial to complete wetting is dominated by short-range interactions, the effect of the long-range forces in a sequential-wetting scenario is to limit the thickness of the adsorbed film to a finite value even if, above $T_{w,1}$, the short-range forces alone would favor complete wetting. The first-order wetting

*Corresponding author. FAX: +49 6151 16-6526. v.weiss@theo.chemie.tu-darmstadt.de

transition thus becomes a first-order thin-thick transition. Its exact location, however, is still largely determined by the temperature at which the effect of the short-range interaction changes from preventing complete wetting to supporting a thick wetting layer. Once the thick film has been formed, the substrate-liquid interface is essentially decoupled from the liquid-vapor interface of the adsorbate [8]. The weak interaction between these two interfaces is solely due to long-range forces. The leading term of these interactions is determined by the Hamaker constant W, which is positive if the two interfaces attract (limited film thickness) and negative if the interfaces repel (diverging film thickness). Right at $T_{w,c}$, the Hamaker constant changes sign. The variation of W with temperature is well described within Dzyaloshinskii-Lifshitz-Pitaevskii (DLP) theory [9] used in conjunction with Israelachvili's simplifications [10] to the dielectric spectra of the media involved [1–3]. In all cases considered, this approach is able to predict the location of $T_{w,c}$ to within a few degrees centigrade. Strictly speaking, however, the temperature at which the Hamaker constant changes sign, T_0, just provides a lower bound to the critical wetting transition temperature $T_{w,c}$ [11]. Taking the true dielectric spectra of all media into account, the interface potential which is shown in Eq. (1) and which was effectively employed in Refs. [1–3] is valid only for relatively thin films (such as the mesoscopic ones considered in this paper), but might have a much more complicated form when retardation effects come into play. The actual interface potential may then change sign several times as the film thickness is increased. Fenzl illustrates the consequences of this scenario and calculates a global wetting phase diagram for a two-oscillator model of the frequency-dependent dielectric permittivity [11]. His model, however, was not applied to the alkane-water systems which are the subject of the present paper and, therefore, no direct comparison is possible at this point. Within the framework of Israelachvili's approximation, the Hamaker constant changes sign only once and we identify the temperature at which this change occurs with $T_{w,c}$.

Upon approaching the critical wetting temperature $T_{w,c}$ in the frustrated complete wetting state, the film thickness l diverges and the contact angle θ vanishes. The asymptotic behavior of these two quantities can be described by power laws. For the film thickness, one has $l \sim (T_{w,c}-T)^{\beta_s}$, while the vanishing of the contact angle is related to the singularity of the surface free energy density by $f \sim 1-\cos\theta \sim |T_{w,c}-T|^{2-\alpha_s}$. It follows that, asymptotically, $\theta \sim (T_{w,c}-T)^{1-\alpha_s/2}$.

In long-range critical wetting, the theoretically expected numerical values of these exponents are $\alpha_s=-1$ and $\beta_s=-1$ [12–14]. They will be observable only in the asymptotic limit, i.e., sufficiently close to the critical wetting temperature. Further away from the critical wetting point, one may still use the functional form of a power law to relate the film thickness or the contact angle, respectively, to the difference $(T_{w,c}-T)$, but one will, in general, not obtain the asymptotic values of the exponents. Instead, effective local exponents, which we denote by α_{eff} and β_{eff}, will be found, the numerical values of which depend on the distance from the critical wetting temperature.

In this paper, we set out to calculate the effective exponents α_{eff} and β_{eff} as functions of the distance from the critical wetting temperature, which is defined as $\tau=(T_{w,c}-T)/T_{w,c}$. The motivation for this study is provided by the puzzling experimental observation that the theoretically predicted exponent of $\beta_{\mathrm{expt}}=-1$ was found from film-thickness measurements in the system of pentane on water [1], while the seemingly very similar systems of hexane on brine yielded exponents that differed considerably from the expected value [2]. In particular, an exponent of $\beta_{\mathrm{expt}}=-0.73\pm0.2$ was deduced from the data for hexane on a 1.5 molar (M) solution of NaCl, while $\beta_{\mathrm{expt}}=-0.57\pm0.19$ was found for hexane on a 2.5M salt solution. In addition, contact-angle measurements on the latter system yielded a value of $\alpha_{\mathrm{expt}}=0.1\pm0.2$ [4], which is very different from the theoretical value of $\alpha_s=-1$. By monitoring the effective local exponents in our calculation, we hope to be able to shed some light on these unexpected experimental results.

The remainder of the paper is organized as follows: In Sec. II, we briefly outline the methodology adopted to calculate the film thickness and the contact angle for pentane on water and for hexane on brine from the long-range interactions alone. These in turn are obtained from the dielectric properties of the isolated media. The results of these calculations as well as the effective exponents deduced from them are shown and discussed in Sec. III. The main conclusions are summarized in Sec. IV.

II. METHODOLOGY

The calculation of the film thickness of a mesoscopically thick layer of liquid alkane, which is present in the frustrated complete wetting state, is based on the asymptotic behavior of the long-range interactions between substrate and adsorbate. It is thus assumed that the liquid layer of adsorbate is sufficiently thick for short-range interactions to be unimportant and for the long-range interaction to determine the film thickness. According to Cahn's theoretical picture, the short-range forces concern only the first layer of adsorbed alkane molecules, i.e., those which are located within a distance of one molecular diameter σ from the substrate surface [15]. Beyond this distance, only the long-range forces (which were not accounted for in Cahn's original theory) affect the adsorbate particles. In the frustrated complete wetting regime, the film thickness l is much (at least ten times) larger than the molecular diameter, for which a numerical value of $\sigma=4.1$ Å is obtained in the case of pentane and of $\sigma=4.4$ Å in the case of hexane from the excluded-volume term in the respective Peng-Robinson equation of state used to describe the thermodynamic properties of the alkane [3,16]. Both conditions mentioned above should, therefore, be met, which means that the free energy (per unit area) can be expanded in terms of the small parameter σ/l, and the resulting series may be truncated after the linear term [17]. The contribution to the free energy per unit area resulting from the long-range interaction (interface potential) within this approximation is

$$\gamma_{\mathrm{LR}}(l,\sigma) = -\frac{W}{12\pi l^2} + \frac{B\sigma}{12\pi l^3}, \tag{1}$$

where W denotes the Hamaker constant and B is the amplitude of the next-to-leading term. These two quantities are

calculated for pentane on pure water and for hexane on brine, respectively, as described in the following two sections. The film thickness and the contact angle can be found from Eq. (1) as explained in Sec. II C.

A. Pentane on water

The Hamaker constant of the three-layer system consisting of water (1), liquid pentane (3), and vapor (2) is given by [10]

$$W = \frac{3}{4} k_B T \Delta_{31}(0) \Delta_{32}(0) + \frac{3}{8\sqrt{2}} \hbar \omega_e N(3,1,3,2), \tag{2}$$

where the abbreviations

$$\Delta_{ik}(0) = \frac{\varepsilon_i(0) - \varepsilon_k(0)}{\varepsilon_i(0) + \varepsilon_k(0)}, \tag{3}$$

$$N(f,g,j,k) = \frac{(n_f^2 - n_g^2)(n_j^2 - n_k^2)}{(n_f^2 + n_g^2)^{1/2}(n_j^2 + n_k^2)^{1/2}[(n_f^2 + n_g^2)^{1/2} + (n_j^2 + n_k^2)^{1/2}]} \tag{4}$$

have been used, and k_B is Boltzmann's constant, while $\hbar$ denotes Planck's constant. To arrive at the above formula for W, Israelachvili's simplifications of the dielectric spectra of water and pentane have been invoked [10], namely, the assumptions that all media involved have the same characteristic absorption frequency ω_e and that the dielectric spectrum of substance j can be represented by $\varepsilon_j(i\zeta) = 1 + (n_j^2 - 1)/[1 + (\zeta/\omega_e)^2]$, with n_j being the refractive index and ζ denoting the frequency; $\varepsilon_j(0)$ is the static dielectric permittivity of substance j.

To calculate the amplitude of the next-to-leading term B, a four-layer structure comprised of water (1), dense liquid pentane (4), regular liquid pentane (3), and vapor (2) is considered. The presence of layer 4 allows one to obtain B within the current theoretical framework and is motivated by the observation that, right at the water-pentane interface, there is a thin layer (of approximately one molecular diameter thickness) of pentane whose density is higher than the bulk liquid density at the same temperature [13,18]. The region of more densely packed alkane close to the surface of a substrate was found by means of ellipsometry in the study of the wetting behavior of alkane on a silicon wafer [19]; Pfohl and Riegler assumed a similar layer of dense alkane to be present also for alkanes on water. In addition, the profiles of the alkane density resulting from a Cahn-type theory [20] indicate a noticeable increase of the density of the liquid alkane near the substrate surface. This preliminary mean-field theory estimates the density to be enhanced by about 12% compared to the bulk density of the liquid [18,21]. The changes in the dielectric properties that result from the higher density are calculated using the Clausius-Mossotti and Lorenz-Lorentz equations [10], respectively.

Within Bertrand's approximation [21], B is obtained as

TABLE I. Representative equations for the dielectric properties of water, brine, the liquid alkanes (pentane and hexane), and the vapor phase. In addition to the relative static dielectric permittivity $\varepsilon(0)$ and the refractive index n, a characteristic absorption frequency common to all media of $\nu_e = \omega_e/(2\pi) = 3 \times 10^{15}$ s^{-1} has been used. T denotes the absolute temperature in K, and c_{NaCl} is the concentration of NaCl in mol liter^{-1}.

Medium	Relative static dielectric permittivity $\varepsilon(0)$
Water [23]	$249.21 - 0.79069\ \mathrm{K}^{-1} T + 0.72997 \times 10^{-3}\ \mathrm{K}^{-2} T^2$
Brine [30]	$\varepsilon_{\mathrm{water}}(0) - 11\ \mathrm{liter\ mol}^{-1}\ c_{\mathrm{NaCl}}$
Pentane [24]	$1.844 - 0.00160\ \mathrm{K}^{-1}(T - 293.15\ \mathrm{K})$
Hexane [24]	$1.890 - 0.00155\ \mathrm{K}^{-1}(T - 293.15\ \mathrm{K})$
Vapor	≈ 1

Medium	Refractive index n
Water [25]	$1.33436 - 1.50585 \times 10^{-5}\ \mathrm{K}^{-1}(T - 273.15\ \mathrm{K}) - 1.94586 \times 10^{-6}\ \mathrm{K}^{-2}(T - 273.15\ \mathrm{K})^2 + 5.23889 \times 10^{-9}\ \mathrm{K}^{-3}(T - 273.15\ \mathrm{K})^3$
Brine [21]	$n_{\mathrm{water}} + 0.00918\ \mathrm{liter\ mol}^{-1}\ c_{\mathrm{NaCl}}$
Pentane [26]	$n_{\mathrm{water}} + 0.034058 - 0.00047645\ \mathrm{K}^{-1}(T - 273.15\ \mathrm{K})$
Hexane [26]	$n_{\mathrm{water}} + 0.049 - 0.0004\ \mathrm{K}^{-1}(T - 273.15\ \mathrm{K})$
Vapor	≈ 1

$$B \approx \frac{3}{2} k_B T \Delta_{32}(0) \Delta_{41}(0) + \frac{3}{4\sqrt{2}} \hbar \omega_e N(3,2,4,1). \tag{5}$$

Other approximate formulas for B have been derived [22], but the resulting numerical differences are very small.

Table I contains the representative equations for the dielectric properties involved in the above expressions for W and B. The dielectric data for the corresponding isolated phases have been taken from various sources [23–26], which are indicated in the table.

Furthermore, in the actual calculations of the film thickness and the contact angle, we use representative equations for the amplitudes W and B, which were obtained by linear regressions to the results of Eqs. (2) and (5):

$$W = -5.308 \times 10^{-23}\ \mathrm{J\ K}^{-1}(T - 273.15\ \mathrm{K}) + 2.763 \times 10^{-21}\ \mathrm{J}, \tag{6}$$

$$B\sigma = -5.621 \times 10^{-32}\ \mathrm{J\ m\ K}^{-1}(T - 273.15\ \mathrm{K}) + 6.618 \times 10^{-30}\ \mathrm{J\ m}. \tag{7}$$

B. Hexane on brine

For the description of the long-range interactions in the system of hexane on salt water, a five-layer model has been suggested [22]. The additional layer, as compared to the four-layer model of alkanes on pure water, is a region near the brine-alkane interface which is significantly depleted of ions; in our simple model, it is even assumed to be pure water. Within the traditional Onsager-Samaras picture of the

interface of electrolyte solutions, such a repulsion of ions from the interface is caused by image charges arising from the sudden variation of the dielectric permittivity at the water-air interface [27]. An alternative view, which is probably more appropriate in concentrated solutions of salt, is that the depletion layer is nothing but the hydration shell of the ions, which keeps them from penetrating to the interfacial region [28]. In any case, the five-layer model consisting of brine (1), water (4), dense liquid hexane (5), liquid hexane (3), and vapor (2) has proved useful in the description of the sequential wetting scenario of hexane on brine [4,22,29]. If the thickness l of the layer of liquid alkane is very much larger than the thickness of the depletion layer δ, which is the case in the frustrated complete wetting state since $l \geq 50$ Å, while $\delta \approx 2$ Å [22], the formulas derived for the five-layer model simplify effectively to the ones of the four-layer model described above for pentane on pure water, the only difference being that the substrate phase, which was pure water in the previous case, is now replaced by brine. The dielectric properties of the depletion layer are, thus, irrelevant.

The Hamaker constant is obtained as before, i.e., from Eq. (2). Replacing the labels in Eq. (5) as appropriate, the amplitude of the next-to-leading term is calculated from

$$B \approx \frac{3}{2} k_B T \Delta_{32}(0) \Delta_{51}(0) + \frac{3}{4\sqrt{2}} \hbar \omega_e N(3,2,5,1). \tag{8}$$

The dielectric properties required to evaluate the above expressions for the different phases have been taken from the literature [21,23–26,30] and are compiled in Table I.

For hexane on brine, the functions $W(T)$ and $B(T)$ exhibit a more pronounced curvature than the ones in the case of pentane on water, for which linear fits, Eqs. (6) and (7), were sufficient. Quadratic fits, however, describe the data accurately, and we use the representative equations

$$W = 5.400 \times 10^{-26}\ \text{J K}^{-2}(T - 273.15\ \text{K})^2 - 5.010 \times 10^{-23}\ \text{J K}^{-1}(T - 273.15\ \text{K}) + 3.025 \times 10^{-21}\ \text{J}, \tag{9}$$

$$B\sigma = 2.944 \times 10^{-35}\ \text{J m K}^{-2}(T - 273.15\ \text{K})^2 - 5.535 \times 10^{-32}\ \text{J m K}^{-1}(T - 273.15\ \text{K}) + 7.663 \times 10^{-30}\ \text{J m} \tag{10}$$

for a salt concentration of $1.5M$ and

$$W = 5.851 \times 10^{-26}\ \text{J K}^{-2}(T - 273.15\ \text{K})^2 - 4.902 \times 10^{-23}\ \text{J K}^{-1}(T - 273.15\ \text{K}) + 2.022 \times 10^{-21}\ \text{J}, \tag{11}$$

$$B\sigma = 3.351 \times 10^{-35}\ \text{J m K}^{-2}(T - 273.15\ \text{K})^2 - 5.441 \times 10^{-32}\ \text{J m K}^{-1}(T - 273.15\ \text{K}) + 6.783 \times 10^{-30}\ \text{J m} \tag{12}$$

for the $2.5M$ solution of NaCl in the actual calculations of the film thicknesses and contact angles.

C. Film thickness and contact angle

The film thickness l is calculated from its asymptotic form following from Eq. (1) for large values of l, namely,

$$l \approx \frac{3B\sigma}{2W}. \tag{13}$$

If B is assumed to be independent of temperature, while W is known to vanish linearly near $T_{w,c}$, i.e., $W \sim |T_{w,c} - T|$, then $\beta_s = \beta_{\text{eff}} = -1$ follows rigorously. If, however, B shows a temperature dependence as well, then β_{eff} will be a function of the distance from the critical wetting temperature.

The contact angle can be found from the amplitudes of the long-range terms alone in the limit of large film thicknesses as well. Using the above expression for the asymptotic film thickness, it is given by [29]

$$1 - \cos\,\theta = \frac{W^3}{81\pi\gamma_{\text{lv}}(B\sigma)^2}, \tag{14}$$

where γ_{lv} is the interfacial tension of the liquid-vapor interface of the adsorbate. This result has been derived by expressing the spreading coefficient S as an integral of the disjoining pressure $\Pi(l)$, which is a function of the layer thickness l. This connection between S and $\Pi(l)$ leads to an exponent relation that involves α_s, β_s, and the exponent m which characterizes the algebraic decay of the long-range interface potential. One finds

$$2 - \alpha_s = 1 - (m-1)\beta_s. \tag{15}$$

This relation was derived by Henderson on the basis of sum rules [31]. For nonretarded van der Waals interactions, one has $m=3$; if retardation effects determine the decay of the interactions, $m=4$.

It is important to recognize the limits of the validity of Eq. (15). It is valid specifically only for long-range critical wetting, and only in the mean-field or weak-fluctuation regimes [32]. Indeed, the derivation supposes that the Hamaker constant W vanishes linearly at the critical wetting transition, i.e., $W \sim (T_{w,c} - T)$, which gives rise to the first term (the "1") on the right-hand side of Eq. (15). This assumption has no analog, for instance, in the strong-fluctuation regime for critical wetting in the presence of short-range forces, for which it is known that the transition does *not* occur at the point at which the leading amplitude of the mean-field interface potential vanishes [33,34].

Another point to stress is that, although α_s and β_s are interrelated through Eq. (15) for a given algebraic decay of the long-range interface potential, the two exponents are truly independent; this fact is most convincingly appreciated by recalling the exponent relation

$$\alpha_s + 2\beta_s + \gamma_s = 2, \tag{16}$$

the surface analog of the Widom-type scaling relation associated with the rigorous Rushbrooke inequality $\alpha + 2\beta + \gamma \geq 2$ for the bulk critical exponents.

The reason for emphasizing Eq. (15) is that the relation may be tested whenever estimates of α_s and β_s are available, such as the effective exponents α_{eff} and β_{eff} which are the subject of this paper.

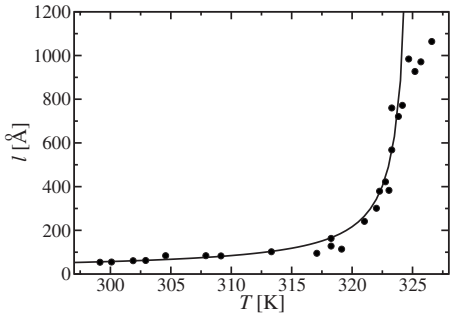

FIG. 1. Film thickness l in the frustrated complete wetting state of pentane on pure water as a function of temperature T. The circles represent experimental data [1], while the continuous line shows the results of the current theory.

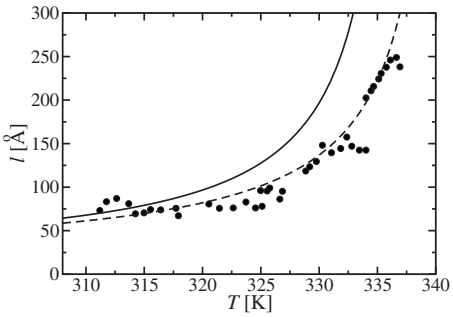

FIG. 2. Film thickness l in the frustrated complete wetting state of hexane on a 1.5M solution of NaCl as a function of temperature T. The circles represent experimental data [2], while the continuous line shows the results of the current theory. The dashed curve is obtained by shifting the continuous one, thereby adjusting the critical wetting temperature to $T_{w,c}=342.05$ K.

To evaluate Eqs. (13) and (14), we use Eqs. (6) and (7) for pentane on water, Eqs. (9) and (10) for hexane on a 1.5M NaCl solution, and Eqs. (11) and (12) for hexane on a 2.5M solution of NaCl in the actual calculations.

The effective exponents α_{eff} and β_{eff} are found from the calculated film thicknesses $l(T)$ and contact angles $\theta(T)$ by taking numerical derivatives of $\log l$ and $\log(1-\cos\theta)$, respectively, with respect to $\log\tau$, where the reduced temperature scale is defined by $\tau=(T_{w,c}-T)/T_{w,c}$. The critical wetting temperature is the temperature at which the Hamaker constant changes sign, i.e., $W(T_{w,c})=0$. Formally, one may write

$$\beta_{\text{eff}}(\tau_0) = \left.\frac{d\log l}{d\log\tau}\right|_{\tau_0}, \tag{17}$$

$$2-\alpha_{\text{eff}}(\tau_0) = \left.\frac{d\log(1-\cos\theta)}{d\log\tau}\right|_{\tau_0}. \tag{18}$$

While the asymptotic values α_s and β_s are obtained in the limit $\tau_0\to 0$, the above derivatives are taken at a finite reduced temperature τ_0; in this case, effective (local) values of the exponents at the corresponding τ_0 are obtained.

III. RESULTS AND DISCUSSION

The results of the film-thickness calculations for pentane on pure water are shown in Fig. 1 and compared with the experimental data of Ragil *et al.* [1]. The agreement between theory (continuous line) and experiment (circles) is excellent up to film thicknesses of 800 Å. For even thicker films, both theory and experiment face problems. Retardation effects, which alter the exponents in the algebraic decay of the long-range interactions, are not accounted for by the current theory; these effects, however, are expected to become important for interactions across distances of hundreds of angstroms. The analysis of the experimentally determined ellipticity and the subsequent conversion into the corresponding film thickness are hampered by the limited validity of Drude's formula, which can only be used for $l<600$ Å [21]. Problems related to retardation are of no concern for the film-thickness data of hexane on brine as these were taken only for $l<300$ Å.

Figure 2 shows the calculated film thickness (continuous line) of hexane on a 1.5M solution of NaCl as a function of temperature. The experimental data of Shahidzadeh *et al.* [2] are represented by circles. Due to the different critical wetting temperatures in the theory and in the experiment (see Table II), there is a clearly visible discrepancy between the data sets. If one adjusts the critical temperature of the calculated data to $T_{w,c}=342.05$ K (dashed curve), which corresponds to a simple shift of the continuous curve, it is seen that the functional form of the divergence in the theory is adequate to describe the experimental findings. The effective exponent β_{eff} is therefore expected to be determined quite accurately from the calculations.

Figure 3 shows the corresponding film-thickness data for hexane on a 2.5M solution of NaCl (continuous line), which are compared with the experimental data taken by Shahidzadeh *et al.* [2]. The critical wetting transition temperatures within theory and experiments are even more different than those for the system of hexane on a 1.5M solution of NaCl; consequently, there are substantial deviations of the calculated values from the experimentally determined ones (cf. also [4]). A temperature shift of the theoretical data by 8 K, corresponding to an apparent $T_{w,c}$ of 324.7 K (dashed line), leads to a reasonably good agreement with the experimental data. The latter do not show as smooth and continuous a divergence of the film thickness as the ones for pentane on water and for hexane on a 1.5M solution of NaCl. In this case, it is, thus, difficult to decide whether or not the calculated effective exponents will be accurate enough to relate to the experimental ones in a meaningful way.

TABLE II. Critical wetting temperatures $T_{w,c}$ in K for pentane on pure water and for hexane on aqueous solutions of NaCl (concentration given in parentheses). The sources of the experimental data are given in square brackets.

System	$T_{w,c}$ (experimental)	$T_{w,c}$ (calculated)
Pentane on water	326.25 [1]	325.4
Hexane on brine (1.5M)	341.05 [2]	338.05
Hexane on brine (2.5M)	321.15 [2], 314 [35]	316.7

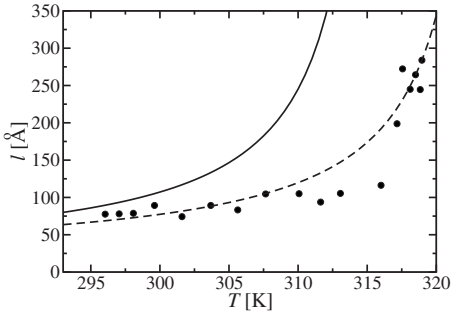

FIG. 3. Film thickness l in the frustrated complete wetting state of hexane on a 2.5M solution of NaCl as a function of temperature T. The circles represent experimental data [2], while the continuous line shows the results of the current theory. The dashed curve is obtained by shifting the continuous one, thereby adjusting the critical wetting temperature to $T_{w,c}=324.7$ K.

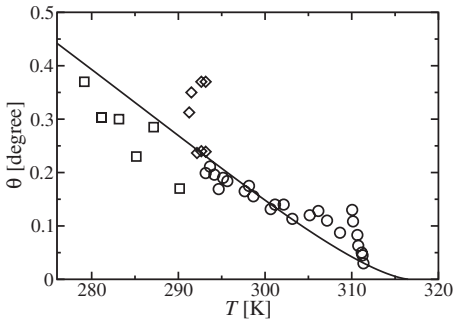

FIG. 4. Contact angle θ for hexane on a 2.5M solution of NaCl as a function of temperature T. The symbols represent experimental data [4], of which some are considered to be in the frustrated complete wetting state (circles), others in the partial wetting state (diamonds), and the remaining ones in the frustrated complete wetting state, but metastable (squares). The continuous line shows the results of the current theory for the frustrated complete wetting state.

There are several possible explanations for the deviations of the temperature at which the calculated Hamaker constant W changes sign from the experimentally observed critical wetting transition temperature $T_{w,c}$. A fundamental reason has already been alluded to in the Introduction, namely, that the temperature at which the Hamaker constant changes sign is only a lower bound to $T_{w,c}$ [11]. The observed discrepancies between theory and experiment are consistent with this statement. Furthermore, by invoking Israelachvili's simplifications to the dielectric spectra of the involved media, many approximations are introduced [10], and it is remarkable that the location of the critical wetting transition is determined with such an accuracy. Additionally, our estimates of W can hardly be better than the quality of the data for the dielectric properties that we use as input and which are compiled in Table I. In particular, we assume the brine phase to show the same variations of the static dielectric permittivity and of the refractive index with temperature as pure water. This assumption alone might explain the observed discrepancies. It should also not be forgotten that the experimental values are somewhat uncertain, too, as will be illustrated in the next paragraph.

The contact angle in the frustrated complete wetting regime is displayed as a function of temperature for hexane on a 2.5M solution of NaCl in Fig. 4. The continuous line follows from the theoretical calculations, while the open symbols are experimental data [4]. The data represented as circles are considered to have been taken in the stable frustrated complete wetting state, i.e., for $T>T_{w,1}\approx 292$ K [4]. The squares correspond to a metastable frustrated complete wetting situation (the continuation of this wetting state to temperatures below $T_{w,1}$) and the diamonds to the partial wetting state, which is stable below $T_{w,1}$. The effective exponent describing the experimental data, α_{expt}, was deduced using only the data represented by the circles. The agreement of the theoretical results and the experimental data for the contact angle is quite satisfactory. It is noteworthy that the critical wetting transition temperature deduced from the contact-angle measurements [4,35] is well below the one found from the film-thickness data [2]; more specifically, the critical wetting transition is found to occur at 314 K, which is to be contrasted with 321 K for the film-thickness data (see Table II). The theoretical value of $T_{w,c}=316.7$ K lies between the two experimental results.

The effective exponents α_{eff} and β_{eff}, which describe the local behavior of the contact angle and the film thickness, respectively, as a function of the distance from the critical wetting temperature, are shown in Fig. 5. Plotted are the theoretical results for pentane on water (continuous lines), for hexane on a 1.5M solution of NaCl (dashed lines), and for hexane on a 2.5M solution of NaCl (dotted lines). In each case, the thick line corresponds to the local exponent α_{eff}, while the thin line shows the local value of β_{eff}. It is seen that an asymptotic value of $\alpha_s=-1$ or $\beta_s=-1$, respectively, is obtained in all cases. There are, however, similarities and differences regarding the way in which these values are approached by the three systems. In all three cases and for both properties, the asymptotic value is approached from above, but the value of α_{eff} deviates from α_s visibly already relatively close to the critical wetting temperature, whereas a

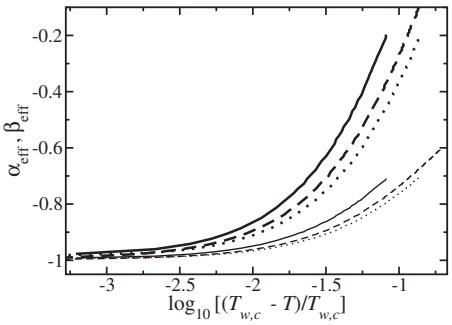

FIG. 5. Effective local exponents α_{eff} and β_{eff} as functions of the reduced temperature. For both exponents, -1 marks the asymptotic value. The three thick curves are for the exponent α_{eff} (contact angle), the thin ones for the exponent β_{eff} (film thickness). In each case, the continuous curve results from calculations for pentane on pure water, the dashed one is for hexane on a 1.5M solution of NaCl, and the dotted one for hexane on a 2.5M solution of NaCl.

more substantial distance from $T_{w,c}$ is required to see deviations of β_{eff} from β_s. A second observation is that, for both α_{eff} and β_{eff}, the deviation from the asymptotic values of the exponents at a given distance from $T_{w,c}$ is more pronounced for pentane on water than for hexane on a 1.5M solution of NaCl, which in turn shows a stronger deviation than hexane on a 2.5M solution of NaCl. This order is exactly the opposite of what was to be expected on grounds of the experimentally deduced exponents β_{expt}: for pentane on water, $\beta_{\text{expt}}=-0.99\pm0.3$ [1,17] was found, while $\beta_{\text{expt}}=-0.73\pm0.2$ for hexane on a 1.5M solution of NaCl and $\beta_{\text{expt}}=-0.57\pm0.19$ for hexane on a 2.5M salt solution [2]. The comparison of effective exponents for different properties of a given system is more favorable: from the film-thickness measurements [2] and the contact-angle measurements [4] for hexane on a 2.5M salt solution, the findings of $\beta_{\text{expt}}=-0.57\pm0.19$ and of $\alpha_{\text{expt}}=0.1\pm0.2$ already suggest that deviations from the asymptotic values of the exponents should be more pronounced for the contact angle than for the film thickness. This observation is consistent with the theoretical results.

In order to understand the apparently opposite trends of β_{expt} and β_{eff} as deduced from experiments and from our theory, respectively, in the three systems, we take a closer look at the temperature ranges in which the different experiments were actually carried out. One finds that the data for pentane on water [1] were taken in a region of $\tau=(T_{w,c}-T)/T_{w,c}\geq10^{-3}$, while the film-thickness measurements for the two systems of hexane on brine [2] were carried out for $\tau\geq10^{-2}$, i.e., further from $T_{w,c}$. In all cases, the exponents were deduced from data covering a temperature range of approximately one order of magnitude in terms of τ above the lower limit quoted above. Interestingly, in the contact-angle measurements, which show the largest discrepancy with respect to the asymptotic value, the temperature range in which the experiments were done was limited to $\tau>10^{-1.5}$. It is, therefore, no longer surprising that the effective and averaged local exponent determined in the experiment, $\alpha_{\text{expt}}=0.1\pm0.2$, differs greatly from the asymptotic value of $\alpha_s=-1$. In view of the fact that the film-thickness data for hexane on brine were taken further away from $T_{w,c}$ than those for pentane on water, it is also quite understandable that the latter yield an exponent β_{expt} which is close to the asymptotic one, while the effective exponents for the systems of hexane on brine show substantial deviations from $\beta_s=-1$. Note again in this context that deviations of β_{eff} from the asymptotic value $\beta_s=-1$ are due to the temperature dependence of the amplitude B.

From the calculated effective exponents displayed in Fig. 5, it becomes clear that the experimentally observed exponents are compatible with the theoretical results if their uncertainties and the temperature range in which they were recorded are taken into account. Averaging the calculated values of β_{eff} and α_{eff} over one order of magnitude of τ in the respective regions appropriate to the experiments on the different systems, one finds $\beta_{\text{eff,av}}=-0.97$ for pentane on water, $\beta_{\text{eff,av}}=-0.82$ for hexane on a 1.5M solution of NaCl, and $\beta_{\text{eff,av}}=-0.86$ for hexane on a 2.5M salt solution. Only the latter falls slightly out of the range of the experimental error margin. For the effective exponent describing the contact-angle data, one finds $-0.76<\alpha_{\text{eff}}<-0.3$ in the range $10^{-1.5}<\tau<10^{-1}$, indicating that large positive deviations from the asymptotic value of $\alpha_s=-1$ are possible if the measurements are done far away from $T_{w,c}$.

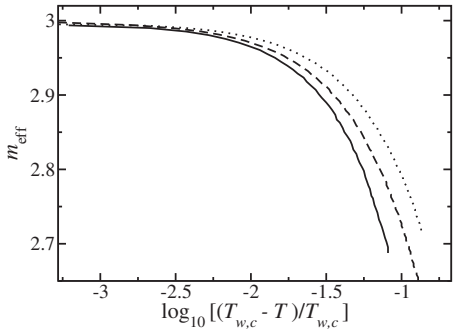

FIG. 6. Effective exponent m_{eff} for the decay of the long-range interface potential as a function of the reduced temperature. This exponent is deduced from the respective values of α_{eff} and β_{eff} using the exponent relation Eq. (15). The continuous curve is for pentane on water, the dashed one for hexane on a 1.5M solution of NaCl, and the dotted one for hexane on a 2.5M solution of NaCl.

When the exponent relation Eq. (15) is invoked with α_{eff} and β_{eff} instead of α_s and β_s, we obtain values for the effective exponent m_{eff}, which are plotted in Fig. 6 as a function of the same temperature variable as the effective exponents in Fig. 5. It is seen that the value of m_{eff} remains near its asymptotic value of $m=3$ over a wide temperature range; this is in strong support of the internal consistency of our approximation scheme, which assumes that we are dealing with nonretarded van der Waals forces. Note that, even at a temperature as far away from $T_{w,c}$ as $\tau=10^{-1.5}$, the deviation of m_{eff} from the value 3 is at most 3%. Moreover, when the experimental findings for α_s and β_s are examined, one sees that, in agreement with earlier statements [36], Eq. (15) is satisfied with values of m remarkably close to 3, which is a strong indication that nonretarded van der Waals forces dominate the scenario of long-range critical wetting also in the experiments.

Note that there is no meaningful way of checking the validity of Eq. (16) using the effective exponents since independently determined values of γ_s, or γ_{eff}, are not available. The only point that we can note here is that, in order for Eq. (16) to remain approximately valid for the effective exponents, the value of γ_{eff} would have to change dramatically and in the right direction (i.e., decrease) to compensate for the changes in α_{eff} and β_{eff}, which are both increasing when moving away from the wetting temperature.

IV. CONCLUSION

The effective exponents describing the divergence of the film thickness, β_{eff}, and the vanishing of the contact angle, α_{eff}, in the frustrated complete wetting state of the sequential-wetting scenarios of pentane on water and of hexane on brine have been calculated based on a two-term expansion of the tails of the long-range interactions between adsorbate and substrate, Eq. (1). The relevant amplitudes in

this expansion are the Hamaker constant W and the next-to-leading term B, both of which are calculated within DLP theory using Israelachvili's simplified formulas and experimental dielectric data (see Table I) for the isolated media. The divergence of the film thickness l and the vanishing of the contact angle θ upon approaching the critical wetting temperature $T_{w,c}$ are asymptotically characterized by power laws: $l \sim (T_{w,c}-T)^{\beta_s}$ and $\theta \sim (T_{w,c}-T)^{1-\alpha_s/2}$. The asymptotic values of the exponents in these power laws, $\beta_s=-1$ and $\alpha_s=-1$, are recovered for temperatures close to the respective critical wetting temperature $T_{w,c}$. Further from $T_{w,c}$, larger (less negative) values are obtained for both effective (apparent) exponents, α_{eff} and β_{eff}, and it is found that α_{eff} increases faster than β_{eff} with increasing distance from $T_{w,c}$. The results are summarized in Fig. 5 and indicate that one can find effective local exponents that are very different from the asymptotic values if the measurements are carried out in a temperature range that is sufficiently far away from $T_{w,c}$. What exactly "far away from $T_{w,c}$" means depends on the property that is measured and, to a lesser extent, on the system of interest. Once again, we would like to stress that local deviations of the effective exponents from their asymptotic values are caused by the temperature dependence of the amplitude B; if B were constant, then α_{eff} would equal α_s and β_{eff} would equal β_s for as long as W varied linearly with temperature.

The theoretical results obtained in this paper are compatible with the available experimental data (within their respective uncertainties) if one takes into account the temperature range in which the data were measured. It had been suspected that the apparent deviations from the asymptotic values are attributable to the effects of higher-order terms in the expansion of the interface potential (the long-range interaction), i.e., terms beyond those given in Eq. (1). It is intriguing to observe that if, for whatever reason, the amplitude B were small (or strictly zero) and the next term in the expansion of $\gamma_{\text{LR}}(l,\sigma)$, proportional to l^{-4}, dominated over it, the resulting asymptotic exponents should be $\alpha_s=0$ and $\beta_s=-1/2$, corresponding to long-range tricritical wetting [31,37]. These exponents are, therefore, also compatible with the experimentally observed values for the exponents in the case of hexane on a 2.5M solution of NaCl [2,4,36], and it is conceivable that the first example of long-range tricritical wetting was seen in the experiments. Note that the above values of α_s and β_s satisfy the exponent relation Eq. (15) with $m=3$ too. It is, however, not obvious why B should be small (or zero) in the above system, but not for pentane on water. Our explicit calculations, based on Eq. (8), do not indicate any significant difference between the two systems. From our current analysis in terms of effective exponents, we see no compelling reason for incorporating higher-order terms into Eq. (1) at present. This is not to say that these terms are definitely of no importance, and the observation of long-range tricritical wetting is still a possibility that cannot be ruled out, but more accurate experimental data would be needed to demonstrate convincingly that these higher-order terms are indeed necessary to describe the frustrated complete wetting state reliably.

ACKNOWLEDGMENTS

We would like to thank Jim Henderson for bringing the possibility of long-range tricritical wetting to our attention. Furthermore, V.C.W. gratefully acknowledges financial support from the German Research Foundation (Deutsche Forschungsgemeinschaft) under Grants No. WE 2540/3-1 and No. WE 2540/3-2, while J.O.I. benefited from FWO Project No. G.0483.04.

[1] K. Ragil, J. Meunier, D. Broseta, J. O. Indekeu, and D. Bonn, Phys. Rev. Lett. **77**, 1532 (1996).
[2] N. Shahidzadeh, D. Bonn, K. Ragil, D. Broseta, and J. Meunier, Phys. Rev. Lett. **80**, 3992 (1998).
[3] E. Bertrand, H. Dobbs, D. Broseta, J. Indekeu, D. Bonn, and J. Meunier, Phys. Rev. Lett. **85**, 1282 (2000).
[4] S. Rafaï, D. Bonn, E. Bertrand, J. Meunier, V. C. Weiss, and J. O. Indekeu, Phys. Rev. Lett. **92**, 245701 (2004).
[5] J. O. Indekeu, K. Ragil, D. Broseta, D. Bonn, and J. Meunier, in *New Approaches to Problems in Liquid State Theory*, edited by C. Caccamo, J. P. Hansen, and G. Stell, NATO Advanced Studies Institute, Series C: Mathematical and Physical Sciences (Kluwer, Dordrecht, 1999), Vol. 529, pp. 337–344.
[6] E. Bertrand, D. Bonn, D. Broseta, and J. Meunier, J. Pet. Sci. Eng. **24**, 221 (1999).
[7] Y. Melean, N. Bureau, and D. Broseta, SPERE **6**, 244 (2003).
[8] V. C. Weiss and B. Widom, Physica A **292**, 137 (2001).
[9] I. E. Dzyaloshinskii, E. M. Lifshitz, and L. P. Pitaevskii, Adv. Phys. **10**, 165 (1961).
[10] J. N. Israelachvili, *Intermolecular and Surface Forces* (Academic Press, London, 1985).
[11] W. Fenzl, Europhys. Lett. **64**, 64 (2003).
[12] S. Dietrich and M. Schick, Phys. Rev. B **31**, 4718 (1985).
[13] V. B. Shenoy and W. F. Saam, Phys. Rev. Lett. **75**, 4086 (1995).
[14] M. P. Nightingale, W. F. Saam, and M. Schick, Phys. Rev. B **30**, 3830 (1984).
[15] J. W. Cahn, J. Chem. Phys. **66**, 3667 (1977).
[16] H. Dobbs, J. Chem. Phys. **114**, 468 (2001).
[17] J. O. Indekeu, K. Ragil, D. Bonn, D. Broseta, and J. Meunier, J. Stat. Phys. **95**, 1009 (1999).
[18] E. Bertrand, D. Bonn, H. Kellay, B. P. Binks, and J. Meunier, Europhys. Lett. **55**, 827 (2001).
[19] T. Pfohl and H. Riegler, Phys. Rev. Lett. **82**, 783 (1999); T. Pfohl, Ph.D. thesis, Universität Potsdam, 1998.
[20] K. Ragil, D. Bonn, D. Broseta, and J. Meunier, J. Chem. Phys. **105**, 5160 (1996).
[21] E. Bertrand, Ph.D. thesis, Université Pierre et Marie Curie–Paris VI, 2000.
[22] V. C. Weiss and J. O. Indekeu, J. Chem. Phys. **118**, 10741 (2003).
[23] *CRC Handbook of Chemistry and Physics*, 73rd ed., edited by D. R. Lide (CRC, Boca Raton, FL, 1992).
[24] *CRC Handbook of Chemistry and Physics*, 66th ed., edited by

R. C. Weast (CRC, Boca Raton, FL, 1985).
[25] Fit to data taken from Ref. [23].
[26] K. Ragil, Ph.D. thesis, Université Pierre et Marie Curie–Paris VI, 1996.
[27] L. Onsager and N. N. T. Samaras, J. Chem. Phys. **2**, 528 (1934).
[28] Y. Levin and J. E. Flores-Mena, Europhys. Lett. **56**, 187 (2001).
[29] V. C. Weiss and J. O. Indekeu, Fluid Phase Equilib. **222-223**, 269 (2004).
[30] J. B. Hasted, D. M. Ritson, and C. H. Collie, J. Chem. Phys. **16**, 1 (1948).
[31] J. R. Henderson, Mol. Phys. **59**, 1049 (1986).
[32] M. E. Fisher, J. Chem. Soc., Faraday Trans. 2 **82**, 1569 (1986).
[33] E. Brézin, B. I. Halperin, and S. Leibler, Phys. Rev. Lett. **50**, 1387 (1983).
[34] D. S. Fisher and D. A. Huse, Phys. Rev. B **32**, 247 (1985).
[35] S. Rafaï, Ph.D. thesis, Université Paris 7–Denis Diderot, 2004.
[36] S. Rafaï, D. Bonn, and J. Meunier, Physica A **358**, 197 (2005).
[37] C. Ebner, W. F. Saam, and A. K. Sen, Phys. Rev. B **32**, 1558 (1985).